Asian Journal of Chemistry; Vol. 33, No. 6 (2021), 1357-1362

ASIAN JOURNAL OF CHEMISTRY

https://doi.org/10.14233/ajchem.2021.23190

Green Mediated Synthesis of Macroporous Hierarchical CeO_2 Nanoparticles using *Mimosa pudica* Leaf Extract for Humidity Sensing Application

NARASIMHA KULKARNI[1,*], M.C. NAVINDAGI[2], M.V.S. MURALI KRISHNA[1] and SHASHIKANT KUSHNOORE[3]

[1]Department of Mechanical Engineering, Chaitanya Bharathi Institute of Technology, Hyderabad-500075, India
[2]Department of Mechanical Engineering, PDA College of Engineering, Kalaburagi-585102, India
[3]Department of Mechanical Engineering, Koneru Lakshmaiah Education Doundation, Vaddeshwaram-522502, India

*Corresponding author: E-mail: narasimhaafz@gmail.com

Received: 3 March 2021; *Accepted*: 15 April 2021; *Published online*: 5 June 2021; AJC-20368

Metal oxide nanoparticles are popular candidates for chemiresistive sensors application. Cerium oxide (CeO_2) based semiconducting gas sensors have gained rapid interest in recent years. In this study, an environment-friendly green synthesis approach was employed for the synthesis of macroporous CeO_2 nanoparticles using *Mimosa pudica* leaf extract. Later the performance of CeO_2 nanoparticles for humidity sensor is demonstrated. X-ray diffraction studies revealed the cubic fluorite crystal structure with no impurities, scanning electron microscopy analysis revealed the macroporous morphology of CeO_2 hierarchical nanoparticles. Humidity sensing properties were studied using interdigitated electrode coated with CeO_2 nanoparticles. The results showed the sensing response of 0.5 times for 10% RH (relative humidity) and seven times for 90% RH. The response and recovery times were found to be as low as 12 s and 15 s, respectively. The experimental results provided an environment-friendly approach for the synthesis of CeO_2 particles and revealed promising results in humidity sensing application.

Keywords: *Mimosa pudica*, Sensing response, Humidity sensor, Interdigitated electrode, Response time.

INTRODUCTION

In the flourishing industrial era where there is a prime necessity of monitoring operating ambiance and pollutants released to the environment, sensors play a vital role in providing the qualitative and quantitative analysis of chemical effluents [1]. Ambient humidity is one of the crucial factors affecting the performance and efficiency of industrial operations. Hence, humidity sensors are extensively used for keeping a check of ambiance in industries and day today's life [2].

Semiconductor metal oxide gas sensors are the most promising ones among different types such as electrochemical, optical, calorimetric gas sensors, *etc*. because they offer advantages like high sensitivity, durability, low cost, and simplicity in function. A variety of materials are used as sensing material in humidity sensors, such as ceramic [3], organic polymers [4], metal oxide [5], carbon nanotubes [6] and various other composites are tailored and equally used. To know, the general working principle of chemiresistive sensors is the change in impedance of sensing material on exposure to humidity [7].

Nanotechnology offers a unique opportunity to tailor and enhance the overall performance of the above-said materials [8]. Because of their small grain size and large surface area, nanomaterials are advantageous for producing chemical sensors. The properties that attract nanomaterials for sensing applications are the availability of more surface-active sites and stronger absorption and adsorption ability than other materials [9]. As humidity sensing is a surface phenomenon, a material with a high surface area is preferable. Hence, porous materials are gaining importance in chemical sensing applications due to the presence of pores (voids) and ease of creation and functionalization of those voids for specific applications [10].

Among the metal oxide nanoparticles in the lanthanide series, cerium is the second and the most reactive element. By virtue of its electro positivity, cerium exhibits dual oxidation states, Ce^{3+} and Ce^{4+}. Ce^{4+} state is considered as stable over Ce^{3+}, hence cerium oxide or ceria (CeO_2) is the most stable oxide of cerium [11]. Cerium oxide is a popularly used semiconducting material having wide bandgap energy of 3.19 eV and high

exciton binding energy. It is an oxide of singular rare earth element having high crystallographic stability up to its melting point of 2700 ºC in its bulk form [12]. It has found a place in many more applications such as catalysts in chemical processes, solid-state gas sensors, energy storage, cosmetics and renewable energy, *etc*. because of its unique ability to switch between its oxidation states [13].

Cerium oxide nanoparticle has attracted many researchers due to their versatile applications in NH_3 sensors [14], H_2 sensors [15], CH_2O [16], NO_2 [17], *etc*. CeO_2 nanoparticles have been a major player in humidity sensor applications. Xie *et al*. [18] synthesized a CeO_2-ionic liquid hybrid by an easy ionothermal route at a low temperature, which delivered excellent sensing properties and good stability over a broad range. Toloshnaik *et al*. [19] reported CeO_2 sensors fabricated using a spin coating of suspended nanoparticles and obtained promising results. Sikarwar *et al*. [20] reported hexagonal-shaped porous CeO_2-Gd_2O_3-CoO nanocomposite based humidity sensors with a maximum sensitivity of 2.006 μW/%RH and 90% reproducibility.

However, several synthesis approaches such as sol-gel, co-precipitation, flame spray pyrolysis, hydrothermal and microwave were employed for the synthesis of CeO_2 nanoparticles. Among these some techniques are complicated like spray pyrolysis, some are time-consuming like hydrothermal method, some are expensive such as microwave method and many procedures use hazardous chemicals. This scenario urges for easy, low cost and eco-friendly synthetic routes to synthesize industrial level production of nanomaterials [21]. In recent times, the green synthesis approach is shown to be an efficient technique to produce high yields of nanoparticles following an eco-friendly process by eliminating toxic residues. The main advantages of this method are cost-effectiveness, high yield process, and no toxicity [22].

Earlier, attempts have been made to adopt this green synthesis approach for the production of CeO_2 nanoparticles using extracellular compounds of fungi [23], albumen egg [24] and plant extracts made of leaves, stem, seeds, *etc*. [25]. The biomolecules that are present in plant extract act as reducing agents in chemical processes and also biomolecules of interest are made to be capped on nanoparticles in various applications using the green synthesis method. Therefore, the synthesis routes mediated by biocomponents demonstrate an easy, eco-friendly, non-toxic, time-saving and economically viable process [26]. In this work, for the first-time green synthesis of porous cerium oxide nanoparticles using *Mimosa pudica* plant leaf extract has been reported and investigated their performance for humidity sensing application.

EXPERIMENTAL

Preparation of plant extract: *Mimosa pudica* fresh leaves were collected and thoroughly washed with deionized water. Finely cut leaves (20 g) were added to 100 mL of deionized water and boiled at 70 ºC for 2 h. The obtained extract was filtered and collected for further use.

Synthesis of cerium oxide nanoparticles using *Mimosa pudica* leaf extract: Cerium nitrate (3.261 g) was added to 100 mL of *Mimosa pudica* leaf extract and continuously stirred at 80 ºC for 4 h. White precipitate followed with yellowish-brown precipitate was formed. The obtained precipitate was dried in a hot air oven at 80 ºC overnight and annealed at 500 ºC for 2 h.

Humidity sensor preparation: Humidity sensor preparation steps were the same as the method reported by Xie *et al*. [27] and are shown in Fig. 1. The above-synthesized ceria (5 mg) was taken and dispersed in 0.5 mL ethanol. The resulting solution was drop coated on self-designed interdigitated electrodes. It was dried for 1 h at 80 ºC and then used for humidity testing.

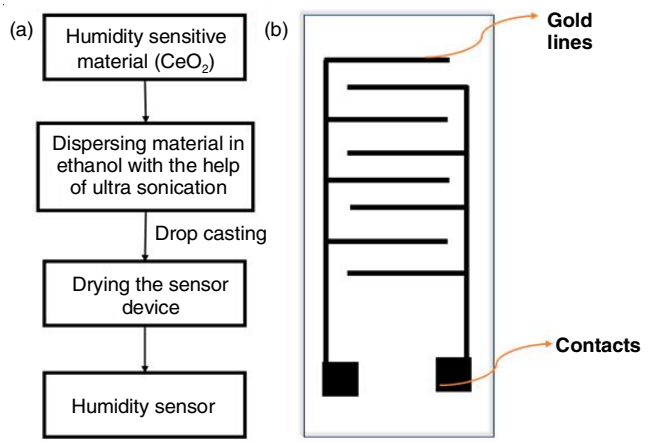

Fig. 1. (a) Steps for humidity sensor preparation, (b) Schematic of interdigitated electrode

Instruments: X-ray spectrometer (Rigaku Ultima-IV) was used to obtain crystallographic information. Morphology of the material was studied using scanning electron microscope (Hitachi SU1510 with W filament). An infrared spectroscope (Perkin-Elmer) was used for detecting functional groups in the range of 4000-400 cm^{-1}. For sensor device, the interdigitated electrode (IDE) with 5 mm × 5 mm dimensions, 10 gold lines with a width of each being 1 mm and separated with 1 mm gap, was fabricated on a glass substrate. The sensor response was measured using a homemade setup connected with mass flow controllers to maintain the required concentration of gas inside the sample chamber. Change in resistance of the material on exposure to different levels of humidity was recorded using Keithly DAQ 6510 digital multi-meter system.

RESULTS AND DISCUSSION

XRD studies: Fig. 2 shows the XRD pattern of green synthesized CeO_2 nanoparticles. It shows the monophasic cubic fluorite structure of CeO_2 (JCPDS 34-0394), in which each Ce^{3+} ion is surrounded by eight oxygen ions. Peaks centered at 28.43º, 32.97º, 47.37º and 56.21º corresponds to (111), (200), (220), (311) and (222) planes, respectively. Particularly obtained Bragg′s peaks are assigned to face-centered cubic structure with a lattice constant of 0.515 nm. By Debye-Scherrer′s approximation, the average crystallite size was calculated to be 9.32 nm.

Surface morphology: Morphological studies of CeO_2 nanoparticles were performed using SEM analysis. Fig. 3 shows

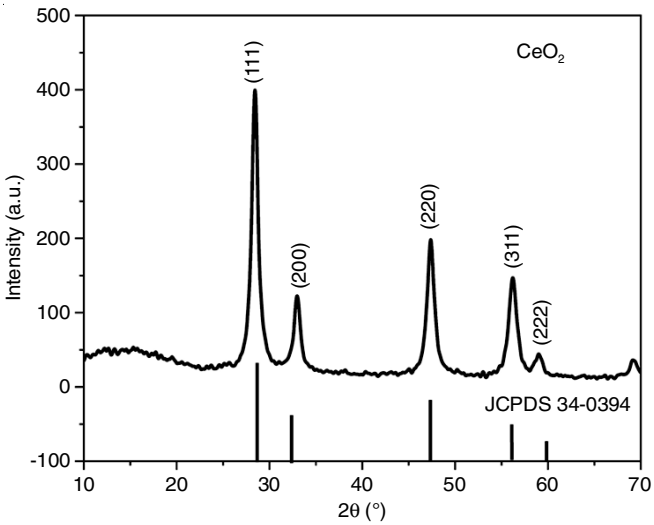

Fig. 2. XRD pattern of CeO_2

the SEM images taken at different magnifications. It was observed that there is no predefined morphology of particles rather irregular particles can be seen. Macroporous hierarchical CeO_2 nanoparticles were obtained as a result of agglomeration during the particle formation to decrease the surface energy of the nanoparticles. It is also evident from the images that the particles consist of macropores, increasing the available area for adsorption of water molecules and have played a vital role in enhanced humidity response of the material.

FTIR studies: The functional groups attached to the material play a notable role in humidity sensing. FT-IR spectra of CeO_2 nanoparticles synthesized from *Mimosa pudica* plant extract is shown in Fig. 4. The absorption band around 3431 cm^{-1} can be attributed to the (O-H) stretching in water molecules attached to CeO_2 nanoparticles [28]. The broad peak at 456 cm^{-1} range corresponds to the Ce-O bond vibrations [29]. An additional band at 1112 cm^{-1} can be associated with the remains of organic species (C-O-H stretching vibration) on the surface CeO_2 nanoparticles [30].

Humidity sensing: The CeO_2 sensor was exposed to five different values of RH, starting from 10% to 90%. It was observed that resistance of the sensor decreased when exposed to humidity. The response was calculated as:

$$\text{Response} = \frac{R_a}{RH} \text{ where } R_a >> RH \quad (1)$$

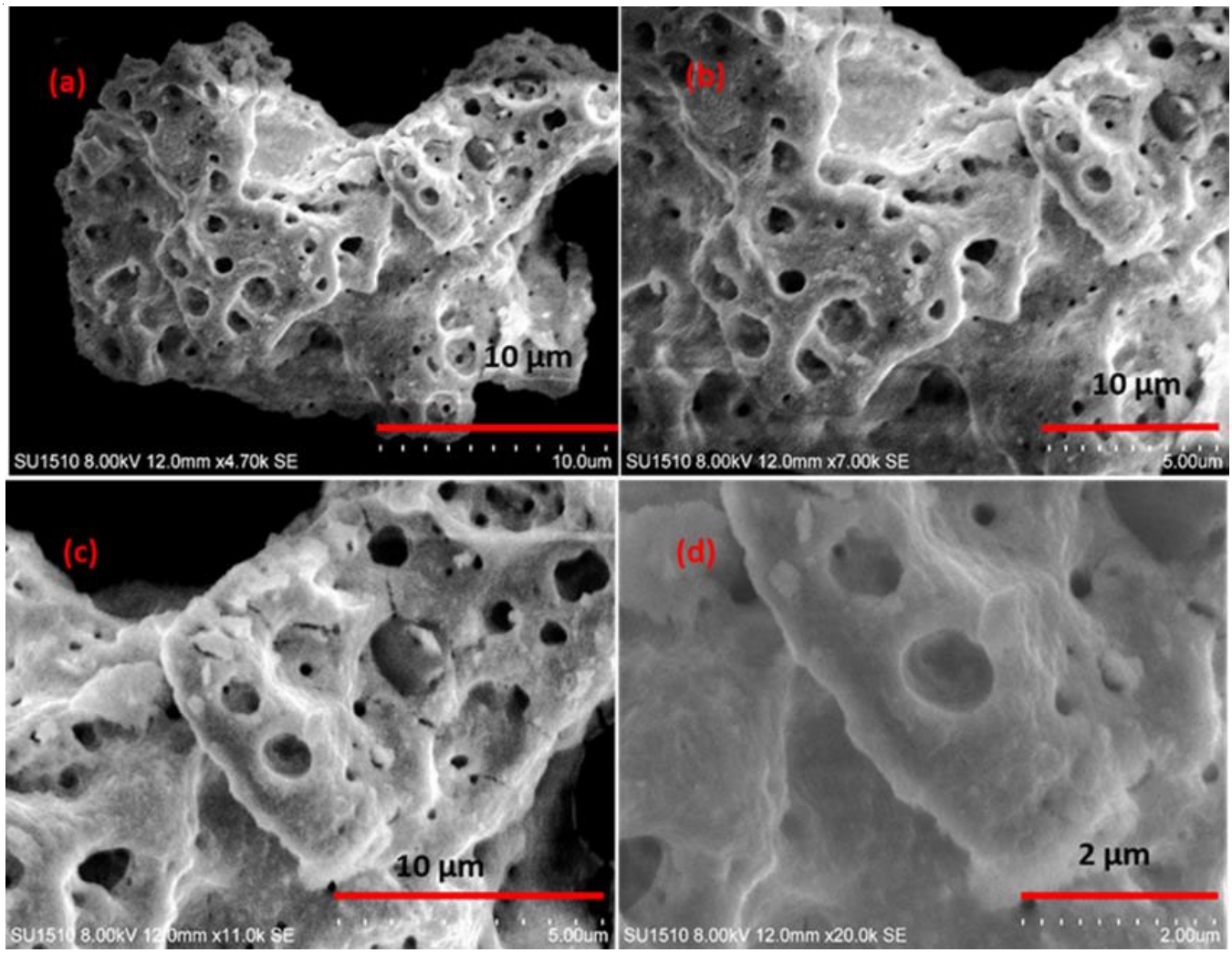

Fig. 3. SEM images of CeO_2 nanoparticles

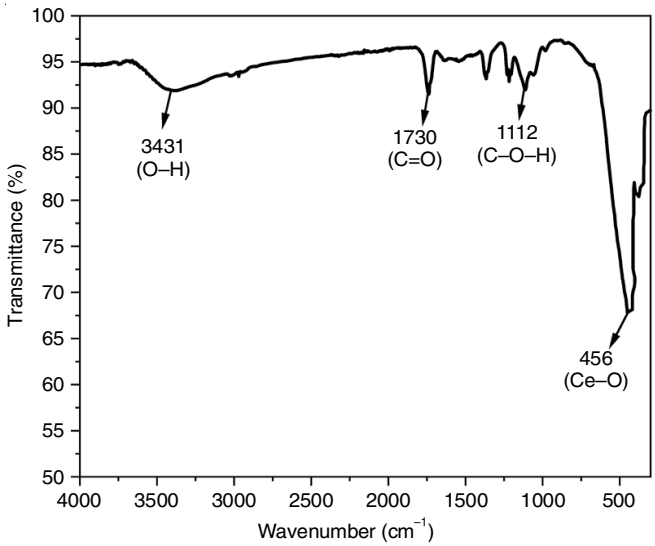

Fig. 4. FTIR spectrum of CeO_2

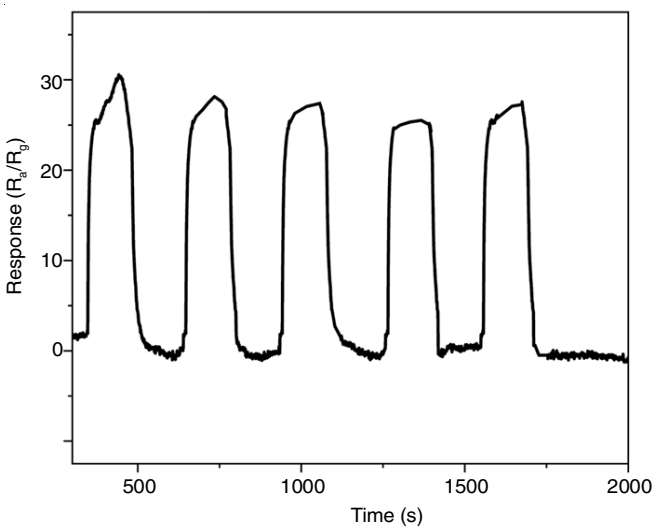

Fig. 6. Repeatability testing for 50% RH

where R_a is the resistance of the sensor device in presence of dry air and RH is the resistance of the sensor when it is exposed to humidity. CeO_2 being an n-type of semiconducting material resistance of the sensor reduced below the baseline resistance on exposure to humidity. Response of the sensor was found around 4 times the baseline for 50% RH and 7.5 times the baseline for 90% RH.

Fig. 5a shows the response of the sensor for five different RH (10%-90%). The response time (time taken by sensor to reach 90% of total response) varied between 33 s (10% RH) to 12 s (90% RH) and recovery time (time taken by the sensor to fall to 10% of total response) found in the range 15 s (10% RH) to 59 s (90% RH). Linear fitted response with respect to humidity is shown in Fig. 5b with an adjacent R^2 value of 0.95.

In order to ensure the repeatability of the sensor, the CeO_2 sensor was exposed to 50% RH to 5 cycles repeatedly. It was found that the response is highly reproducible as seen from reproducibility test results (Fig. 6).

Sensing mechanism: Water adsorption is the main criterion in humidity sensing. The sensor on exposure to humidity for the first time, a single layer of water molecules was formed on the surface of the sensing material. This layer is said to have formed due to chemisorption of water molecules and proton transfer occurs among hydronium ions (H_3O^+) [31]. Certainly, the number of layers of water molecules rises with an increase in humidity (RH) [32]. The secondary layers were formed due to physisorption over the first layer of water molecules. Again, the H_3O^+ ions formed in corresponding layers will act as charge carriers [32]. The proton of one water molecule with H_3O^+ ion is released to the neighboring water molecule and likewise to the next one covering the layer [33]. So according to the Grotthuss mechanism, H^+ can move freely in the physisorbed water layers.

Owing to the fact that Ce^{4+} in CeO_2 has a small ionic radius (101 Pauling radius) forming a high positive charge, the surface of CeO_2 exhibits high charge density. Due to this a strong electric field is induced around CeO_2, ionization of water molecules is augmented and this also influences deeply the physisorbed

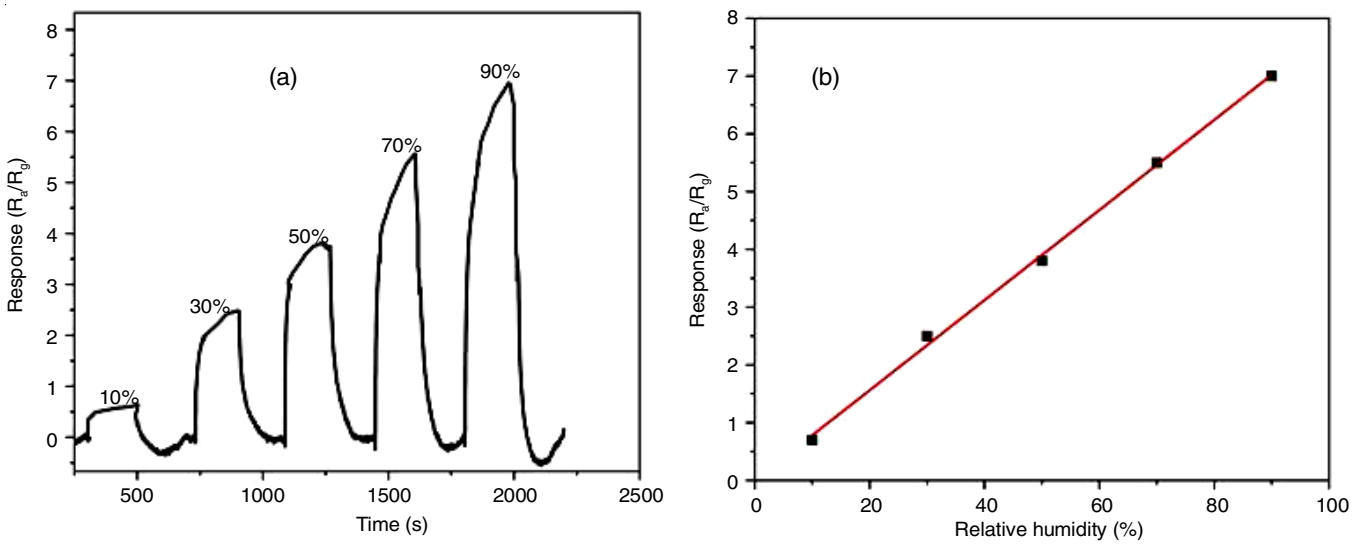

Fig. 5. (a) CeO_2 Humidity sensing response for 5 different RH values, (b) Linear fitting of response

water layers [34]. On the other hand, the large surface to volume ratio of macroporous CeO_2 plays a vital role in conduction and hence increasing the response. The adsorption and desorption of water molecules in macropores are shown in Fig. 7.

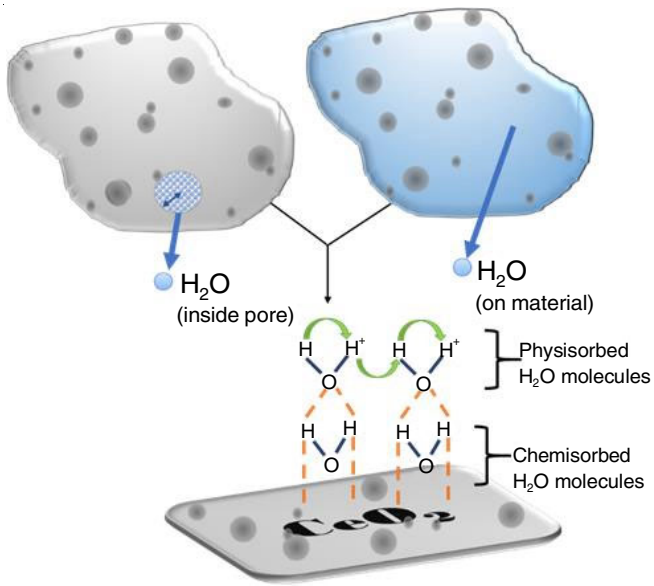

Fig. 7. Sensing mechanism of humidity sensor

Conclusion

Macroporous hierarchical CeO_2 nanoparticles were synthesized for the first time by green-mediated synthesis using *Mimosa pudica* leaf extract. The characterization results showed the successful synthesis of the same. The morphological data from SEM images have provided evidence to infer the porosity distribution throughout the microparticles. The fabricated humidity sensors have realized the linearity relationship with sensing response of 0.5 times for 10% and 7 times for 90% response, good repeatability over 5 cycles for 50% RH. Overall, the results show that the *Mimosa pudica* green mediated synthesis has provided a safe environment-friendly synthesis route to obtain macroporous hierarchical CeO_2 nanoparticles and has the potential to provide efficient results in sensing applications.

ACKNOWLEDGEMENTS

The authors thank Chaitanya Bharathi Institute of Technology, Hyderabad, India for the financial support.

CONFLICT OF INTEREST

The authors declare that there is no conflict of interests regarding the publication of this article.

REFERENCES

1. F. Ejeian, P. Etedali, H.-A. Mansouri-Tehrani, A. Soozanipour, Z.X. Low, M. Asadnia, A. Taheri-Kafrani and A. Razmjou, *Biosens. Bioelectron.*, **118**, 66 (2018); https://doi.org/10.1016/j.bios.2018.07.019
2. Z. Chen and C. Lu, *Sens. Lett.*, **3**, 274 (2005); https://doi.org/10.1166/sl.2005.045
3 T.A. Blank, L.P. Eksperiandova and K.N. Belikov, *Sens. Actuators B Chem.*, **228**, 416 (2016); https://doi.org/10.1016/j.snb.2016.01.015
4. Y. Sakai, Y. Sadaoka and M. Matsuguchi, *Sens. Actuators B Chem.*, **35**, 85 (1996); https://doi.org/10.1016/S0925-4005(96)02019-9
5. N. Rezlescu, E. Rezlescu, C. Doroftei and P.D. Popa, *J. Phys. Conf. Ser.*, **15**, 296 (2005); https://doi.org/10.1088/1742-6596/15/1/049
6. H.W. Chen, R.J. Wu, K.H. Chan, Y.L. Sun and P.G. Su, *Sens. Actuators B Chem.*, **104**, 80 (2005); https://doi.org/10.1016/j.snb.2004.04.105
7. A. Erol, S. Okur, B. Comba, Ö. Mermer and M.Ç. Arikan, *Sens. Actuators B Chem.*, **145**, 174 (2010); https://doi.org/10.1016/j.snb.2009.11.051
8. S. Sharma and M. Madou, *Philos. Trans.- Royal Soc., Math. Phys. Eng. Sci.*, **370**, 2448 (2012); https://doi.org/10.1098/rsta.2011.0506
9. I. Khan, K. Saeed and I. Khan, *Arab. J. Chem.*, **12**, 908 (2019); https://doi.org/10.1016/j.arabjc.2017.05.011
10. Z.M. Wang, Nanoporous Materials, Elsevier Ltd. (2010).
11 A. Younis, D. Chu and S. Li, Cerium Oxide Nanostructures and their Applications, In: Functionalized Nanomaterials, InTech, pp 53-68 (2016); https://doi.org/10.5772/65937
12. N. Thovhogi, A. Diallo, A. Gurib-Fakim and M. Maaza, *J. Alloys Compd.*, **647**, 392 (2015); https://doi.org/10.1016/j.jallcom.2015.06.076
13. A. Dhall and W. Self, *Antioxidants*, **7**, 97 (2018); https://doi.org/10.3390/antiox7080097
14. L. Wang, H. Huang, S. Xiao, D. Cai, Y. Liu, B. Liu, D. Wang, C. Wang, H. Li, Y. Wang, Q. Li and T. Wang, *Appl. Mater. Interf.*, **6**, 14131 (2014); https://doi.org/10.1021/am503286h
15. J. Hu, Y. Sun, Y. Xue, M. Zhang, P. Li, K. Lian, S. Zhuiykov, W. Zhang and Y. Chen, *Sens. Actuators B Chem.*, **257**, 124 (2018); https://doi.org/10.1016/j.snb.2017.10.139
16. S. Hussain, N. Aslam, X.Y. Yang, M.S. Javed, Z. Xu, M. Wang, G. Liu and G. Qiao, *Ceram. Int.*, **44**, 19624 (2018); https://doi.org/10.1016/j.ceramint.2018.07.212
17. J. Hu, C. Zou, Y. Su, M. Li, X. Ye, B. Cai, E.S.W. Kong, Z. Yang and Y. Zhang, *Sens. Actuators B Chem.*, **270**, 119 (2018); https://doi.org/10.1016/j.snb.2018.05.027
18. W. Xie, X. Duan, J. Deng, J. Nie and T. Wang, *Sens. Actuators B Chem.*, **252**, 870 (2017); https://doi.org/10.1016/j.snb.2017.06.093
19. T. Toloshniak, Y. Guhel, A. Besq and B. Boudart, *Microelectron. Eng.*, **207**, 7 (2019); https://doi.org/10.1016/j.mee.2018.11.013
20. S. Sikarwar, B.C. Yadav, R.K. Sonker, G.I. Dzhardimalieva and J.K. Rajput, *Appl. Surf. Sci.*, **479**, 326 (2019); https://doi.org/10.1016/j.apsusc.2019.02.108
21. M. Nyoka, Y.E. Choonara, P. Kumar, P.P.D. Kondiah and V. Pillay, *Nanomaterials*, **10**, 242 (2020); https://doi.org/10.3390/nano10020242
22. N.H.A. Nguyen, V.V.T. Padil, V.I. Slaveykova, M. Èerník and A. Ševcù, *Nanoscale Res. Lett.*, **13**, 159 (2018); https://doi.org/10.1186/s11671-018-2575-5
23. F. Paquin, J. Rivnay, A. Salleo, N. Stingelin and C. Silva-Acuña, *J. Mater. Chem. C Mater. Opt. Electron. Devices*, **3**, 10715 (2015); https://doi.org/10.1039/C5TC02043C
24 C. Nanoparticles, S. Maensiri, C. Masingboon, P. Laokul and W. Jareonboon, V. Promarak, P.L. Anderson and S. Seraphin, *Crystal Growth Des.*, **7**, 950 (2007); https://doi.org/10.1021/cg0608864
25. T.V. Surendra and S.M. Roopan, *J. Photochem. Photobiol. B*, **161**, 122 (2016); https://doi.org/10.1016/j.jphotobiol.2016.05.019
26 V. Pisal, P. Wakchaure, N. Patil and S. Bhagwat, *Mater. Res. Express*, **6**, 115409 (2019); https://orcid.org/0000-0002-9207-5899

27. W. Xie, B. Liu, S. Xiao, H. Li, Y. Wang, D. Cai, D. Wang, L. Wang, Y. Liu, Q. Li and T. Wang, *Sens. Actuators B Chem.*, **215**, 125 (2015); https://doi.org/10.1016/j.snb.2015.03.051
28. S. Vivek, P. Arunkumar and K.S. Babu, *RSC Adv.*, **6**, 45947 (2016); https://doi.org/10.1039/C6RA04120E
29. F.S. Sangsefidi, M. Nejati, J. Verdi and M. Salavati-Niasari, *J. Clean. Prod.*, **156**, 741 (2017); https://doi.org/10.1016/j.jclepro.2017.04.114
30. G. Zhang, X. Shen and Y. Yang, *J. Phys. Chem. C*, **115**, 7145 (2011); https://doi.org/10.1021/jp110256s
31. A. Sun, L. Huang and Y. Li, *Sens. Actuators B Chem.*, **139**, 543 (2009); https://doi.org/10.1016/j.snb.2009.03.064
32. D. Zhang, Y. Sun, P. Li and Y. Zhang, *ACS Appl. Mater. Interfaces*, **8**, 14142 (2016); https://doi.org/10.1021/acsami.6b02206
33. W. Geng, Q. Yuan, X. Jiang, J. Tu, L. Duan, J. Gu and Q. Zhang, *Sens. Actuators B Chem.*, **174**, 513 (2012); https://doi.org/10.1016/j.snb.2012.08.057
34. X.Q. Fu, C. Wang, H.C. Yu, Y.G. Wang and T.H. Wang, *Nanotechnology*, **18**, 145503 (2007); https://doi.org/10.1088/0957-4484/18/14/145503